Case Studies in Construction Materials 22 (2025) e04599

Contents lists available at ScienceDirect

Case Studies in Construction Materials

journal homepage: www.elsevier.com/locate/cscm

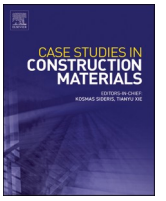

Durability assessment of GFRP bars in concrete exposed to field environment based on interlaminar shear strength

Hiroki Sakuraba [a,b,*], Allan Manalo [a], Omar Alajarmeh [a], Brahim Benmokrane [c]

[a] Centre for Future Materials (CFM), University of Southern Queensland, Toowoomba, QLD 4350, Australia
[b] Innovative Materials and Resources Research Centre, Public Works Research Institute, Tsukuba, Ibaraki 305-8516, Japan
[c] University of Sherbrooke, Department of Civil & Building Engineering, Sherbrooke, Quebec J1K 2R1, Canada

ARTICLE INFO

Keywords:
GFRP bars
Field durability
Interlaminar shear strength
Prediction

ABSTRACT

The interlaminar shear strength (ILSS) can be an indicator of the deterioration of glass fibre-reinforced polymer (GFRP) bars. This property is normally evaluated by using a sample with a length equal to four to seven times the bar diameter, which can be extracted from in-service structures. First, this study conducted an intensive review to establish the relationship between tensile strength (TS) and ILSS retentions of vinyl-ester based GFRP bars, including the effect of sustained stress. TS and ILSS retentions show 0.18–0.92 and 0.30–0.92, respectively, when fibre, resin, and fibre-resin interface damage is observed near the exposed surface. This relationship demonstrates the applicability of assessing the durability of GFRP bars based on ILSS. Available ILSS retentions range from 0.71 to 0.93 on the field durability of GFRP bars extracted from 11- to 20-year-old bridge barriers, bridge decks, a dry-dock, and exposed bars. The reported field durability is compared with a prediction model established from laboratory immersion tests for GFRP bars embedded in concrete. It is shown that predictions based on the immersion in tap water or saline solution in the laboratory can explain the reduction in ILSS of GFRP bars extracted from actual structures while a prediction based on the immersion in alkaline solution is conservative.

1. Introduction

Glass fibre-reinforced polymer (GFRP) bars as reinforcement in concrete structures have been used where steel corrosion is seriously concerned. This is because of chloride ingress causing significant steel corrosion in concrete structures resulting in a numerous attempt for repair, strengthening, and finally replacement to keep them in service [1,2]. Durability is an important issue upon applying GFRP bars having an entirely different degradation mechanism from that of reinforcing steel bars [3,4]. The performance of structural members using GFRP bars have been studied for GFRP bar-concrete interface bond [5,6], beams [7–9], slabs [10–12], columns [13,14], and segments [15]. The significant outcomes of these research and developments have led to the implementation of GFRP bars in actual field applications such as highway bridges [16] and maritime infrastructure [17]. For example, GFRP bars have been commonly used for bridge barriers and decks [16], and boating infrastructure [17]. In terms of material development, the use of thermoplastic as a matrix for GFRP bars has recently been studied since it can allow to be post-formed on site, which can achieve efficient construction, unlike the case of conventional thermoset based GFRP bars [18]. In addition, ultra high-performance engineering cementitious

* Corresponding author at: Centre for Future Materials (CFM), University of Southern Queensland, Toowoomba, QLD 4350, Australia.
E-mail address: Hiroki.Sakuraba@unisq.edu.au (H. Sakuraba).

https://doi.org/10.1016/j.cscm.2025.e04599
Received 16 December 2024; Received in revised form 18 March 2025; Accepted 27 March 2025
Available online 29 March 2025

composites reinforced (UHPC) with GFRP bars have been studied to overcome a relatively low stiffness due to the low elastic modulus of GFRP compared to conventional steel [19]. In these studies, short polyethylene fibres are used for UHPC instead of short steel fibres, resulting in superior durability [20]. Environmentally friendly concrete with GFRP bars has also been studied, such as concrete with a high volume of fly ash that accounting for 50 % of cementitious materials for reducing CO_2 emission [21] and seawater sea-sand concrete to reduce resource depletion of flesh water and sand [22].

In the following part, a review to assess the field durability of GFRP bars based on interlaminar shear strength (ILSS) is shown in the order of (1) the durability of GFRP bars based on tensile strength (TS), (2) the field investigation of GFRP bars based on ILSS, (3) the prediction of ILSS of GFRP bars, (4) the effect of sustained stress on the durability of GFRP bars, (5) object of the present study.

The durability of GFRP bars in an alkaline environment has been widely studied over the last two decades by many researchers [23–26]. This is because when glass fibres are exposed to alkaline solution, they can leach from the surface, whereas carbon fibres, the other typical fibre type, have an inert surface chemistry [27]. Tensile tests after alkaline conditioning are generally conducted as a measure of the durability of GFRP bars for use as internal reinforcement in concrete structures. Chen et al. [23] tested two types of GFRP bars made of two types of E-glass fibres and the same vinyl-ester resin (GFRP1 and GFRP2 bars) by conditioning in an alkaline solution and proposed a prediction procedure based on the Arrhenius relation. It was shown that TS retention of GFRP1 and GFRP2 bars conditioned in alkaline solution with a pH of 13.6 and 12.7 for 120 days at 60℃ were 38 % and 59 %, respectively. As a result of prediction, TS retention of GFRP1 bars dropped to 50 % after only half a year exposure at 20°C, and for GFRP2 bars exposed at 20°C, TS retention was 50 % after about 3 years. Robert et al. [24,25] carried out experiments on concrete-embedded GFRP bars made of E-glass fibres and vinyl-ester resin by conditioning them in tap water and saline solution. The results of their research showed that the durability of the concrete-embedded GFRP bars was less affected by accelerated aging than the bars exposed to an alkaline solution. After conditioning in tap water at 50℃ for 240 days and in saline solution at 50℃ for 365 days, TS retentions were 84 % and 89 %, respectively. More recently, Sun et al. [26] conducted an experimental study on the durability of concrete-embedded GFRP bars made of E-glass fibres and vinyl-ester resin with different diameters of 10, 12, 16, and 25 mm conditioned in seawater. Experimental results showed that after immersion in seawater for 183 days at 60°C, TS retention remained from 52 % to 72 %, with the larger diameter bars having higher TS retention. A prediction based on the experimental results showed that TS retention of the GFRP bars after 100 years was above the standard design values.

The field durability of 11- to 20-year-old GFRP bars by testing ILSS has been studied on a bridge barrier [28] and bridge decks [29, 30] using small dimensioned samples with lengths equal to four to seven times the bar diameter (a length of one diameter greater than the test span) [31]. This is because extracting a large sample with length equal to the free length plus two times the anchor length to test tensile properties from in-service structures is practically impossible. Even only for the free length, more than 380 mm or 40 times the effective diameter of the bars is required [32]. Benmokrane et al. [28] investigated a field durability of GFRP bars made of E-glass fibres and viny-ester resin in a concrete bridge barrier built in Canada in 2004. Samples of the GFRP bars were extracted from the bridge barrier. The short-beam shear test according to ASTM D4475 [31] was carried out and 85 % of ILSS retention was observed. Benzecry et al. [29] and Al-Khafaji et al. [30] presented a durability assessment of 15- to 20-year-old GFRP bars in bridge decks built between 1996 and 2004 in the United States. The eleven bridge decks were investigated, and ILSS retention was evaluated in the two bridge decks where reference samples at the time of construction were available. Results of the short-beam shear test according to ASTM D4475 [31] showed ILSS retention ranging from 73 % to 93 %. Furthermore, Al-Zahrani [33] conducted an exposure test on two types of GFRP bars made of E-glass or ECR-glass fibres and vinyl-ester resins at a tidal zone in Saudi Arabia for 20 years. After exposure, the GFRP bars were extracted from concrete beam specimens, and the short-beam shear test according to ASTM D4475 [31] was carried out. ILSS retention was shown to be between 78 % and 84 %. Micelli and Nanni [34] stated that ILSS may indicate a measure of resin damage caused by the penetration of fluids and may provide an indication of possible impacts on longitudinal properties. The field durability studies have shown that ILSS can be reduced during actual exposure. Nevertheless, the relationship between TS and ILSS of GFRP bars after alkaline conditioning has not been quantitatively shown although several researchers [27,35–43] have tested TS and ILSS in the same experimental programme. In order to demonstrate the reliability of GFRP bars in concrete structures based on the investigation of ILSS, a comprehensive study is needed. Since the durability of GFRP bars depends on the manufacturing process and components such as fibre types, resin, and sizing [27], a review of the relationship between TS and ILSS including a wide variety of GFRP bars is therefore required to assess the field durability of GFRP bars.

In terms of prediction based on ILSS, Yu et al. [44] proposed a prediction model focusing on the relationship between ILSS and water uptake of GFRP bars made of E-glass fibres and epoxy resin after alkaline conditioning. Experimental results showed that ILSS retention was almost 100 % up to 0.6 % of water absorption in the GFRP bars, whereas it was reduced linearly up to 44 % with the range of the water absorption from 0.6 % to 2.0 %. Wang et al. [45] exhibited a prediction model which is focused on ILSS retention of GFRP bars made of E-glass fibres and epoxy resin after alkaline conditioning. It was shown that 42 % and 80 % of ILSS retention was observed after immersion for 84 days at 55°C with a pH of 13.4 and 12.7, respectively. As a result of the prediction with a pH of 13.4 for time to reach 70 % of ILSS retention, 7.0–13.6 years was reported at mean annual temperatures from 3.9 to 9.9°C. Manalo et al. [46] conducted a comprehensive experiment on ILSS of bare GFRP bars and concrete-embedded bars, which are made of ECR-glass fibres and vinyl-ester resin after alkaline conditioning. A prediction method that can assess the durability and long-term performance of GFRP bars in concrete environments was then established. Predicted results at a mean annual temperature of 30°C showed that ILSS of retention was 54 % and 68 % when exposed to alkaline solution and tap water or seawater after 100 years of service, respectively. However, the results of these studies have not been verified with the field data described above.

The effect of sustained stress to GFRP bars is also an important durability issue [47]. Wu et al. [48] presented a long-term durability on GFRP bars made of E-glass fibres and vinyl-ester resin embedded in concrete beam specimens with/without a constant load corresponding to 20 % of the ultimate bending moment. The beam specimens were immersed in an alkaline solution with a pH of 13.0.

Experimental results conditioned for 300 days showed that TS retention was reduced from 82 % to 73 % by applying the constant load. Zeng et al. [49] conducted experiments on the durability of GFRP bars made of glass fibres and vinyl-ester resin in an alkaline solution with a pH of 12.6 for 90 days at 60°C and with a constant load inducing an initial strain of 3500μ in the GFRP bars. The test results showed that TS retention was reduced from 94 % to 88 % by applying the constant load. Furthermore, Zhou et al. [50] tested GFRP bars

Table 1
Experimental database of FRP bars obtained in laboratory.

Study number	Author	Published year	Fibre type and resin system	Bar diameter (mm)	Tensile strength (MPa)	Interlaminar shear strength (MPa)	Fibre content (%)	Alkaline conditioning
1	Kim et al. [35]	2008	E-glass, Vinylester	12.7	693 661	36.9 42.3	73.3 (wt.) 69.1 (wt.)	Alkaline solution, pH13.0, up to 60 days at 40℃
2	Benmokrane et al. [36]	2017	ECR-glass, Vinylester	9.5 12.7 15.9 19.1 25.4	1315 1282 1237 1270 1271	54.7 52.9 55.8 56.0 47.5	80.9 (wt.) 81.8 (wt.) 82.6 (wt.) 82.7 (wt.) 83.0 (wt.)	Alkaline solution, pH12.6, up to 90 days at 60℃
3	Fergani et al. [37]	2018	ECR-glass, Vinylester	8.0	1542	73.0	88.0 (wt.)	Alkaline solution, pH12.7 up to 270 days at RT, 40℃ and 60℃
4	Benmokrane et al. [27]	2020	E-glass, Vinylester (3 types) ECR-glass, Vinylester (2 types) ECR-glass, Vinylester (7 types) Basalt, Vinylester (3 types) Basalt, Polyurethane (2 types) Basalt, Epoxy (2 types) Carbon, Epoxy (2 types) Carbon Vinylester (3 types)	15.0 15.0 13.0 13.0 13.0 13.0 13.0	1324–1440 1061, 1407 1103–1601 1481–1641 1317, 1458 1278, 1427 1576, 1797 1920–1993	45.1–62.6 56.2, 49.4 45.4–70.5 41.7–60.9 49.9, 73.6 51.6, 67.3 67.6, 67.2 43.2–60.2	77.5–80.6 (wt.) 78.8, 81.2 (wt.) 78.2–80.0 (wt.) 78.5–84.2 (wt.) 79.8, 78.7 (wt.) 77.0, 78.2 (wt.) 71.4, 74.2 (wt.) 69.7, 68.7 (wt.)	Alkaline solution, pH13.0, up to 90 days at 60℃
5	Ali et al. [38]	2020	Basalt, Vinylester	9.5 12.7 15.9 19.0 25.0	1240 1050 1388 1508 1023	58.0 52.0 53.0 42.0 49.0	80.4 (wt.) 80.3 (wt.) 82.6 (wt.) 82.4 (wt.) 79.6 (wt.)	Alkaline solution, pH12.8, up to 90 days at 60℃
6	Morales et al. [39]	2021	ECR-glass, Vinylester	9.5	1220	44.9	85.1 (wt.)	Embedded in concrete, and immersed in seawater, up to 24 months at 60℃
7	Lu et al. [40]	2022	E-glass, Epoxy	6.0	939	27.2	76 (vol.)	Embedded in concrete, and immersed in artificial seawater, up to 120 days at RT, 40℃, and 60℃
8	Delaplanque et al. [41]	2024	Glass* , Vinylester	10.0	1128	45.6	N/A	Embedded in concrete, and immersed in alkaline solution, pH13.5, up to 540 days at 20, 40, 60℃
9	Feng et al. [42]	2024	Basalt, Epoxy	8.0	1585	54.9	65 (vol.)	Embedded in normal and low alkalinity concrete, and immersed in artificial seawater, up to 180 days at 55℃
10	Guo et al. [43]	2024	Basalt, Epoxy	10.0	1215	45.0	65 (vol.)	Embedded in seawater sea sand concrete, and immersed in seawater, up to 360 days at 55℃

Note: the type of glass fibre (E- or ECR-glass) is not shown in the literature [41]

made of glass fibres and vinyl-ester resin embedded in ultra-high-performance engineered cementitious composites (UHP-ECC) which have a compressive strength of more than 100 MPa and low porosity. After immersion in an alkaline solution with a pH of 12.6 for 180 days at 40℃, sustained loads induced microcracks in UHP-ECC covers, resulting in reduced protection of the GFRP bars, despite the superior property of UHP-ECC. Despite the efforts of these studies, the effect of sustained stress on ILSS of GFRP bars has not yet been exhibited.

This study conducts an intensive review of the relationship between TS and ILSS retentions of GFRP bars to show the applicability of assessing the field durability of GFRP bars based on ILSS, supported by microscopic observations. The review also includes an evaluation of the effect of sustained stress on the relationship since it is inherent in actual concrete structures. The results of field investigations and long-term predictions are then compared and discussed. A prediction method developed by other researchers [46] is used for the evaluation, which can consider the effect of temperature, immersion agent, and concrete cover. The results of this study will provide a better understanding of the correlation between TS and ILSS retentions of GFRP bars after alkaline conditioning even under sustained stress. Verification of the predicted results with field exposure results will provide a useful indicator of the in-service durability of GFRP bars in actual reinforced concrete infrastructure.

In this context, the structure of this paper is as follows: In Section 2, an experimental database is explained to discuss the relationship between TS and ILSS retentions of a wide variety of GFRP bars including other FRP bars. In Section 3, a discussion based on the database shows that there is a relationship between TS and ILSS retentions of GFRP bars by analysing them quantitatively, while the review in Section 1 has shown the overview of TS and ILSS retentions. In Section 4, the ILSS retention of GFRP bars exposed in the field is compared with the predicted results based on the fact that the relationship between TS and ILSS retentions exists.

2. Experimental database

Vinyl-ester based GFRP bars are commonly used in concrete structures [28], which were the focus of the present study. However, for a better understanding of the correlation between TS and ILSS retentions of vinyl-ester based GFRP bars after alkaline conditioning, a comprehensive review of laboratory experimental work to evaluate the strength retention of FRP bars, including basalt fibre-reinforced polymer (BFRP) bars and carbon fibre-reinforced polymer (CFRP) bars, was conducted. In order to construct a reliable database, experimental data consisting of fibre type and resin system, bar diameter, strengths, fibre content and alkaline condition method were collected, which are related to the degradation of FRP bars. For field data, the experimental work on vinyl-ester based GFRP bars was compiled with exposure conditions and information on concrete. These are summarized in the following sections.

2.1. Laboratory data

A summary of the experimental database of FRP bars is shown in Table 1. For comparison with GFRP bars, experimental data of BFRP bars and CFRP bars are also included. In these research, TS and ILSS tests in accordance with ASTM D3916 [51] or ASTM D7205 [32], and ASTM D4475 [31], respectively, were carried out for both reference samples and conditioned samples, so that TS and ILSS retentions can be obtained. In tensile tests, GFRP bars with anchors or grips are mounted in a mechanical testing machine and monotonically loaded up to failure while force, longitudinal strain, and longitudinal displacement are recorded [32]. Failure of GFRP bars within the gauge length is required, and therefore fibre rupture is a typical failure mode. Note that if a significant proportion of failures occur within or just outside an anchor or grip, the means of introducing force into the bar is required to be reconsidered [32]. In interlaminar shear tests (short beam tests), GFRP bars are deflected until shear failure occurs at the mid-plane of the horizontally supported bar while force is recorded [31]. Note that ASTM D 4475 suggests adjusting the span to achieve the required shear failure [31].

In study No.1, Kim et al. [35] conducted an experiment on two types of GFRP bars (nominal diameters 12.7 mm) conditioned in an alkaline solution with a pH of 13.0 for 60 days at 40°C. In study No.2, Benmokrane et al. [36] investigated GFRP bars of five diameters (nominal diameters of 9.5, 12.7, 15.9, 19.1, and 25.4 mm) conditioned in an alkaline solution with a pH of 12.6 for 90 days at 60°. In study No.3, Fergani et al. [37] presented an experimental program on GFRP bars (nominal diameter 8.0 mm) conditioned in alkaline solution with a pH of 12.7 for 270 days at 20, 40, and 60°C. In study No.4, Benmokrane et al. [27] carried out a comprehensive experiment on 24 types of FRP bars (GFRP, BFRP, CFRP, nominal diameters of 13.0 and 15.0 mm) conditioned in alkaline solution with a pH of 13.0 for 90 days at 60°C. In study No.5, Ali et al. [38] tested BFRP bars of five diameters (nominal diameters of 9.5, 12.7, 15.9, 19.0, and 25.0 mm) conditioned in an alkaline solution with a pH of 12.8 for 90 days at 60°C. In study No.6, Morales et al. [39] conducted an experiment on concrete embedded GFRP bars (nominal diameter 9.5 mm), with two types of concrete mix, conditioned in seawater up to 24 months at 60°C. In study No.7, Lu et al. [40] presented an experimental program on concrete embedded GFRP bars (nominal diameter 6.0 mm) conditioned in artificial seawater up to 120 days at room temperature, 40°C and 60°C. This study set prestress at the stress levels of 20 % and 40 % of TS of the GFRP bars during conditioning. In study No.8, Delaplanque et al. [41] examined partially cured GFRP bars (nominal diameter 10.0 mm) embedded in concrete immersed in an alkaline solution with a pH of 13.5 up to 540 days at 20°C, 40°C, and 60°C. It was reported that the initial glass transition temperature (T_g) of the GFRP bars was 71°C while the T_g values after conditioning for 540 days at 20°C, 40°C, and 60°C showed 78°C, 90°C, and 103°C, respectively. The curing ratio of the GFRP bars was not reported as the manufacturer did not disclose characteristic of the resin system. In study No.9, Feng et al. [42] investigated BFRP bars (nominal diameter 8.0 mm) embedded in normal and low alkalinity concrete, conditioned in artificial seawater up to 180 days at 55°C. In study No.10, Guo et al. [43]. tested BFRP bars (nominal diameter 10.0 mm) embedded in seawater sea sand concrete, conditioned in seawater up to 360 days at 55°C. In the tensile tests and interlaminar shear tests, fibre ruptures and horizontal shear failures were stated by [36,38–43] and by [27,36,38–41,43], respectively. It can therefore be assumed that the failure

modes in the database are consistent.

2.2. Field exposure data

A summary of the experimental database of vinyl-ester based GFRP bars obtained from field exposed concrete structures and specimens is shown in Table 2. In these research, ILSS test in accordance with ASTM D4475 [31] was carried out on both reference samples and extracted samples, and therefore ILSS retention can be obtained.

Benmokrane et al. [28] investigated 11-year-old GFRP bars embedded in bridge barrier walls constructed in Quebec, Canada, which were subjected to freeze-thaw cycles and exposure to chlorides from deicing salt. Ramanathan et al. [52] examined 18-year-old GFRP bars embedded in a dry-dock constructed in Hawaii, the United States, which is exposed to seawater. Benzecry et al. [29] and Al-Khafaji et al. [30] assessed 15- and 17-year-old GFRP bars embedded in bridge decks constructed in Texas and Ohio, the United States, which were also subjected to freeze-thaw cycles and exposure to chlorides from deicing salt. Concrete cores were extracted from the bridge barrier walls and bridge decks with a concrete cover of at least 63 mm, where this information was available, and the pH of the concrete cores was measured in the range of 11.5–12.3. Al-Zahrani [33] conducted an exposure test on GFRP bars embedded in concrete beam specimens for 20 years at a tidal zone in Jubail, Saudi Arabia, which were subjected to seawater immersion, wet state, and dry state. GFRP bars were extracted from the specimens with a concrete cover of 25 mm. Fig. 1 shows the bridges and the exposure specimens wherein the above-mentioned GFRP bars were extracted [28,29,33,52]. In the interlaminar shear tests, horizontal shear failures have been reported by several researchers [28,30,33]. However, Ramanathan et al. [52] reported that clear horizontal shear failure was observed in one of four specimens tested, whereas failure of the other specimens presented as horizontal cracks on the outer surface in the region where loading was applied with a coefficient of variation of about 2 %. It should be noted that as the specimens were taken from the field and are of limited length, it was not possible to adjust the span to achieve shear failure as described in ASTM D4475 [31].

3. Comparison of strength retentions of FRP bars after alkaline conditioning

3.1. Relationship between TS and ILSS retentions

Fig. 2 shows the relationship between TS and ILSS retentions of FRP bars without sustained stress, and the legends in Fig. 2 distinguish between fibre type and resin systems. Vinyl-ester, epoxy, and polyurethane resins are described as VE, EP, and PU, respectively. In ECR glass+VE F [39] and ECR glass+VE S [39], the GFRP bars were embedded in fly ash concrete (F) and slag concrete (S), respectively. In the case of GFRP and BFRP, it can be inferred that the reduction of ILSS can be slower than that of TS. In the results of E-glass+VE [35], ECR-glass+VE [27,37], and E-glass+EP [40], TS and ILSS retentions show 0.18–0.92 and 0.30–0.92, respectively. In contrast, in the results of E-glass+VE [27] and ECR glass+VE [36,39], TS retention shows 0.65–0.97 while ILSS retention remains from 0.88 to 1.0. These differences can be attributed to degradation mechanisms in FRP bars typically denoted as (1) fibre dominated; (2) matrix dominated; and (3) fibre-matrix interface dominated or combined mechanisms [54]. Namely, the reduction of TS is governed by fibre, while the reduction of ILSS is governed by resin and fibre-matrix interface. For BFRP, Benmokrane et al. [27] showed that seven types of BFRP tended to have lower ILSS retention after alkaline conditioning than those of 12 types of GFRP. They described that some of BFRP bars having individual fibre diameter of less than 12μm exhibited a certain degree of porosity. The small-diameter fibres could experience issues such as porosity/cracking or uneven fibre distribution. Wang et al. [55] conducted an image analysis, focused on the influence of fibre diameter, on the durability of GFRP and BFRP bars after alkaline conditioning. It was shown that a lower durability of the BFRP bars at high temperature could be partly attributed to smaller diameter of the basalt fibres and that a thinner resin layer surrounding individual basalt fibres was observed compared to that of glass fibres. These findings can explain the lower ILSS retention of BFRP than those of GFRP bars shown in Fig. 2. Fig. 3 shows the relationship between TS and ILSS retentions of FRP bars with different conditioning periods. In Basalt+EP OPC [42] and Basalt+EP LA [42], the GFRP bars were embedded in normal concrete (OPC) and low alkalinity concrete (LA), respectively. It is confirmed that as the conditioning period increase, the TS and ILSS retentions decrease while the relationship remains the same.

The results of durability studies for ECR-glass+VE [37] showed that both of TS and ILSS retentions are reduced. Fergani et al. [37] explained this observation by conducting SEM analysis focusing on the outer layer of the GFRP bars. The SEM revealed that the fibre, resin, and fibre-resin interface were damaged as shown in Fig. 4, which is consistent with the results of the TS and ILSS retentions. With regard to the results of ECR+VE [36] in which the ILSS retention remains higher than TS retention, Benmokrane et al. [36] carried out SEM analysis as shown in Fig. 5 focusing on the centre and surface of the GFRP bars. The SEM showed small debonding between the fibres and matrix near the exposed surface in some conditioned specimens. This damage to the fibre-matrix interface can reduce the load transfer between the fibres and result in a reduction in TS. Moreover, Achillides and Pilakoutas [56] stated that when an FRP bar is pulled in tension through the surface, there can be some differential movement between the core and surface fibres, resulting in a higher surface normal stress than that at the core. This shear lag effect caused small debonding at the fibre-matrix interface and even at the surface, which reduced the TS of GFRP bars. These results highlight that when the fibre, resin, and fibre-resin interface near the exposed surface are damaged, both TS and ILSS can be decreased as shown in Fig. 6(a). Similarly, when the fibre-resin interface near the exposed surface is damaged, TS can be mainly decreased due to the reduction in load transfer between fibres and resin, and the shear lag effect as shown in Fig. 6(b).

The effect of post-curing is evaluated based on the results of the partially cured GFRP bars (see Section 2.1 and Table 1) identified as PaCu Glass+VE [41] which are totally different from the other results of GFRP bars. TS retention of PaCu Glass+VE [41] ranges from

Table 2
Experimental database of GFRP bars obtained in field exposure.

Studynumber	Author	Publishedyear	Fibreandresintype	Bardiameter(mm)	Tensilestrength(MPa)	Interlaminarshearstrength(MPa)	Fibrecontent(%)	Alkalineconditioning	MeanannualTemperature * *(°C)	Rainfall(mm)	Exposureyears	28 − dayconcretecompressivestrength(MPa)	pHofconcrete	Concretecover(mm)
1	Benmokrane et al. [28]	2018	E-glass, Vinylester	15.9	650 *	64.9	78.6 (wt.)	Bridge barrier in Quebec, Canada	4.0	1075	11	50	12.3	65/70
2	Ramanathan et al. [52]	2021	E-glass, Vinylester	15.9	N/A	51.2	73.6 (wt.)	Dry-dock in Hawaii, United States	25	559	18	N/A	N/A	50
2	Benzecry et al. [29] and Al-Khafaji et al. [30]* **	2021	E-glass, Vinylester	19.0	N/A	41.0	76.4 (wt.)	Bridge deck in Ohio, United States	11	968	17	N/A	12.2	63.5
			E-glass, Vinylester	16.0	785	45.0	75.7 (wt.) [53]	Bridge deck in Texas, United States	14	500	15	N/A	11.5	N/A
			E-glass, Vinylester	19.0	N/A	49.0	80.5 (wt.) [53]							
3	Al-Zahrani [33]	2024	E-glass, Vinylester	13.0	745	56.5	N/A	Exposure specimen in Jubail, Saudi Arabia	26	101 (Exposed to tidal zone)	20	55.7	N/A	25
			ECR-glass, Vinylester	13.0	655	46.1	N/A	Exposure specimen in Jubail, Saudi Arabia						

Note: *Guaranteed tensile strength: average tensile strength minus three times standard deviation, ** annual mean temperature from the World Climate & Temperature online database by 8 August 2024. (http://www.climate.top), ***Literatures [29,30] are two-part series. Benzecry et al. [29] and Al-Khafaji et al. [30] presented selected bridges, bar extraction and concrete assessment; and an assessment of GFRP bars, respectively.

(a) Bridge in Québec, Canada [28]

(b) Dry-dock in Hawaii, United States [52]

(c) Bridge in Ohio, United States [29]

(d) Bridge in Texas, United States [29]

(e) Exposed beams in Jubail, Saudi Arabia [33]

Fig. 1. Bridges and exposure specimens having GFRP bars.

0.74 to 1.05 while the ILSS retention shows from 0.95 to 1.31. Delaplanque et al. [41] reported that the effect of post-curing had limited changes in TS while it gave a significant improvement in ILSS. However, this is the case that curing is not enough as described in the T_g values in the Section 2.1. For instance, Morales et al. [39], providing the results of ECR-glass+VE [39], reported that no considerable changes in the T_g value (about 110℃) occurred even after 24 month-conditioning at 60℃. They concluded that the effect of post-curing was not observed since the GFRP bars were exposed to temperature much lower than the T_g value. It is also worth mentioning that the current standard specification [57] requires the T_g value and degree of cure to be greater than 100℃ and 95 % respectively.

Studies on the durability of CFRP bars concluded that the reduction of ILSS can be faster than that of TS. In the results of Carbon+VE [27] and Carbon+EP [27], TS and ILSS retentions shows 0.95–1.00 and 0.61–0.77, respectively. Besides these findings, Benmokrane et al. [27] wherein they immersed different fibre types in an alkaline solution for 168 h at 96℃ conducted SEM analysis. Fig. 7 shows SEM images of each fibre type after alkaline conditioning. It was revealed that the carbon fibre had an inert surface while the other fibres (E-glass, ECR-glass, and basalt) had deteriorated surfaces. Due to this characteristic of the carbon fibre, a poor interfacial adhesion between the carbon fibres and the resins but a strong tensile property was confirmed.

The results from the available literature demonstrated that the TS retention of vinyl-ester based GFRP bars can be assessed based on ILSS retention. It is recommended that for specification, the alkaline resistance of GFRP bars should be assessed not only by TS as

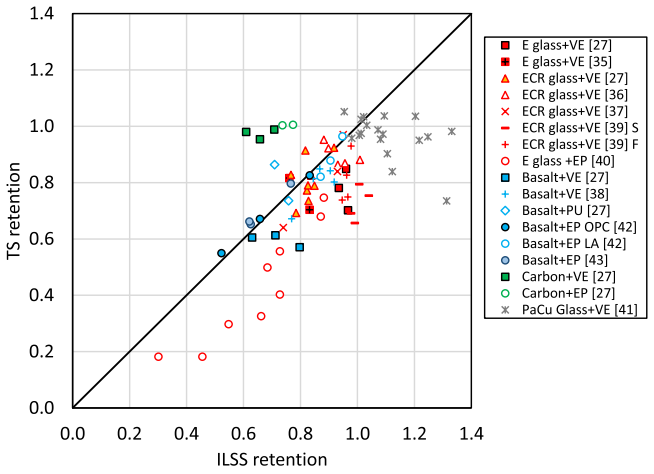

Fig. 2. Relationship between TS and ILSS retentions of FRP bars without sustained stress.

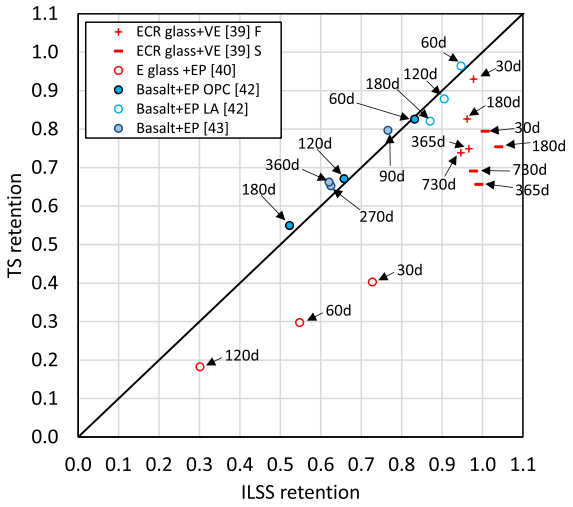

Fig. 3. Relationship between TS and ILSS retentions of FRP bars with different conditioning periods.

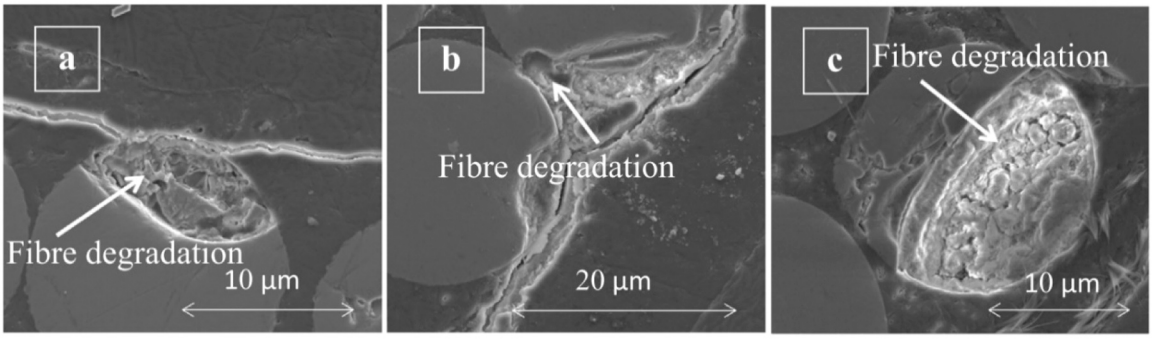

Fig. 4. SEM images showing the degradation in fibre, resin, and fibre-resin near surface of the bar [37].

specified by ASTM 7957 [57] but also by ILSS in terms of assessing the relationship between TS and ILSS retentions. This is because some of the GFRP bars in Fig. 2 showed that the reduction of ILSS is much slower than that of TS. The GFRP bars having the much slower reduction in ILSS cannot be specified by only the types of glass fibres or types of the resin system. The independent samples *t*-test was used to compare the means of ILSS retention between ECR-glass+VE [36] and ECR-glass+VE [27] conditioned for 90 days at 60℃.

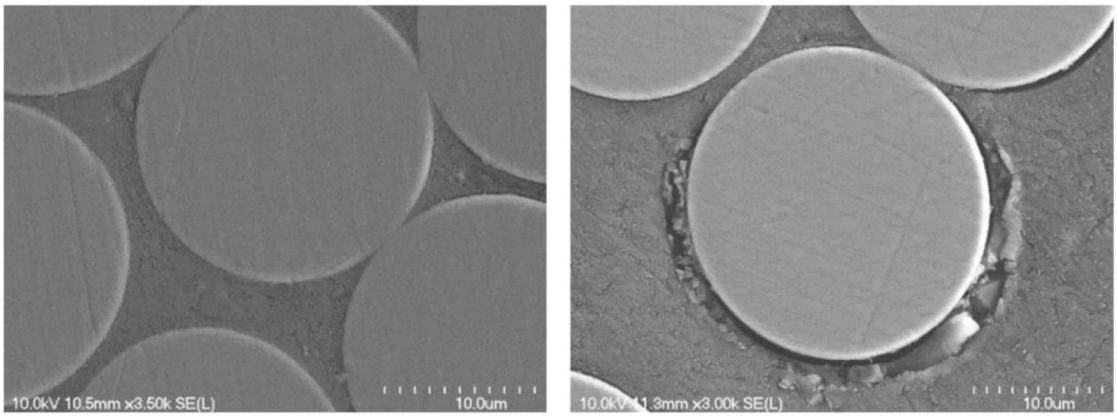

Fig. 5. SEM images showing the degradation in fibre-resin interface: left: centre of the bar; right: near surface of the bar [36].

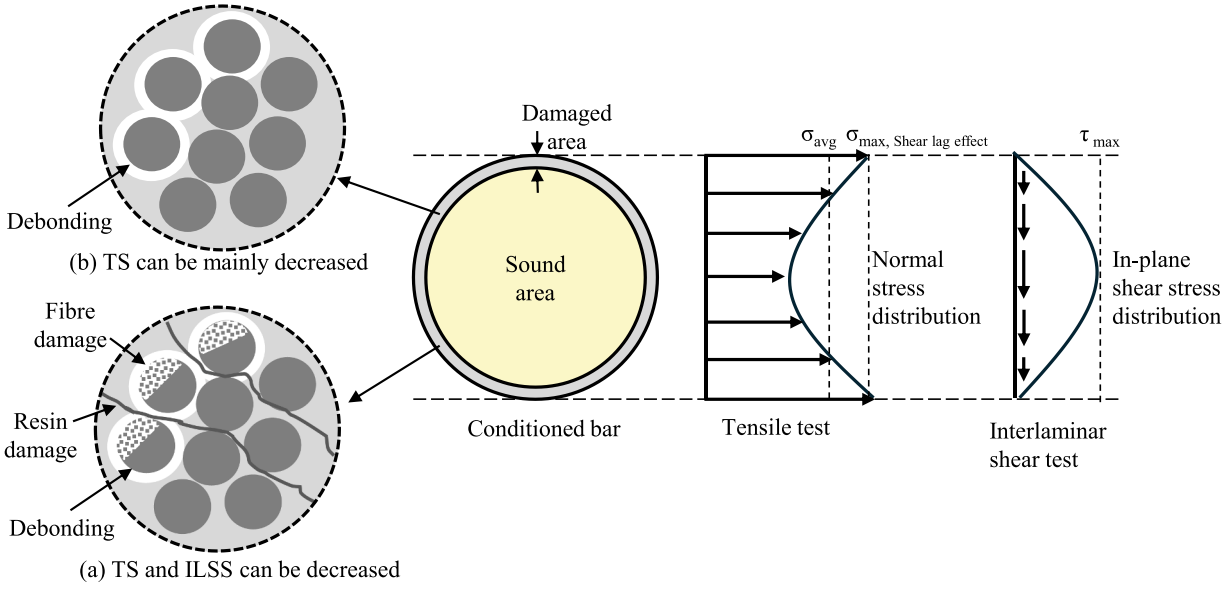

Fig. 6. Damage mechanism to TS and ILSS of FRP bars.

It confirms that there is a statistically significant difference [$t(7) = 4.03, p = 0.002$] between them. Benmokrane et al. [27] stated that the effect of fibre sizing at the manufacturing significantly affects the ILSS of GFRP bars before and after alkaline conditioning. This can explain why the trends among ECR glass+VE [27,36,37,39] are different even for the same type of fibre and resin system. Further study is needed on the effect of fibre sizing to the relationship between TS and ILSS retentions of GFRP bars.

3.2. *Effect of sustained stress*

GFRP bars used as internal reinforcement in actual concrete structures are subjected to sustained stress, and therefore the effect of sustained stress to the relationship between TS and ILSS retentions of GFRP bars is evaluated. Under high levels of stress, micro-cracks in the matrix of GFRP bars can be formed, and they can create a network for the penetration of corrosive agents from the surrounding medium towards the core of the bars [58]. Benmokrane et al. [59] found that three types of stress corrosion mechanisms are identified by an experiment on GFRP bars subjected to sustained stress and alkaline condition: stress dominated, crack propagation dominated, and diffusion dominated. These are evaluated at stress levels of 50–68 %, 35–50 %, and 25–30 % of TS of the GFRP bars, respectively.

Fig. 8 shows the effect of sustained stress on the relationship between TS and ILSS retentions of GFRP bars after alkaline conditioning up to 120 days (see Table 1). The legends in Fig. 8 are distinguished by the temperature and stress levels. It is shown that as the temperature and stress level increase, TS and ILSS retentions decrease. The relationship between TS and ILSS can be kept same as shown in Fig. 2. Chang et al. [60] presented an experimental study on the durability of the seawater sea-sand concrete beam reinforced with GFRP bars made of E-glass fibres and vinyl-ester resin under the combined influence of seawater exposure and sustained load. The

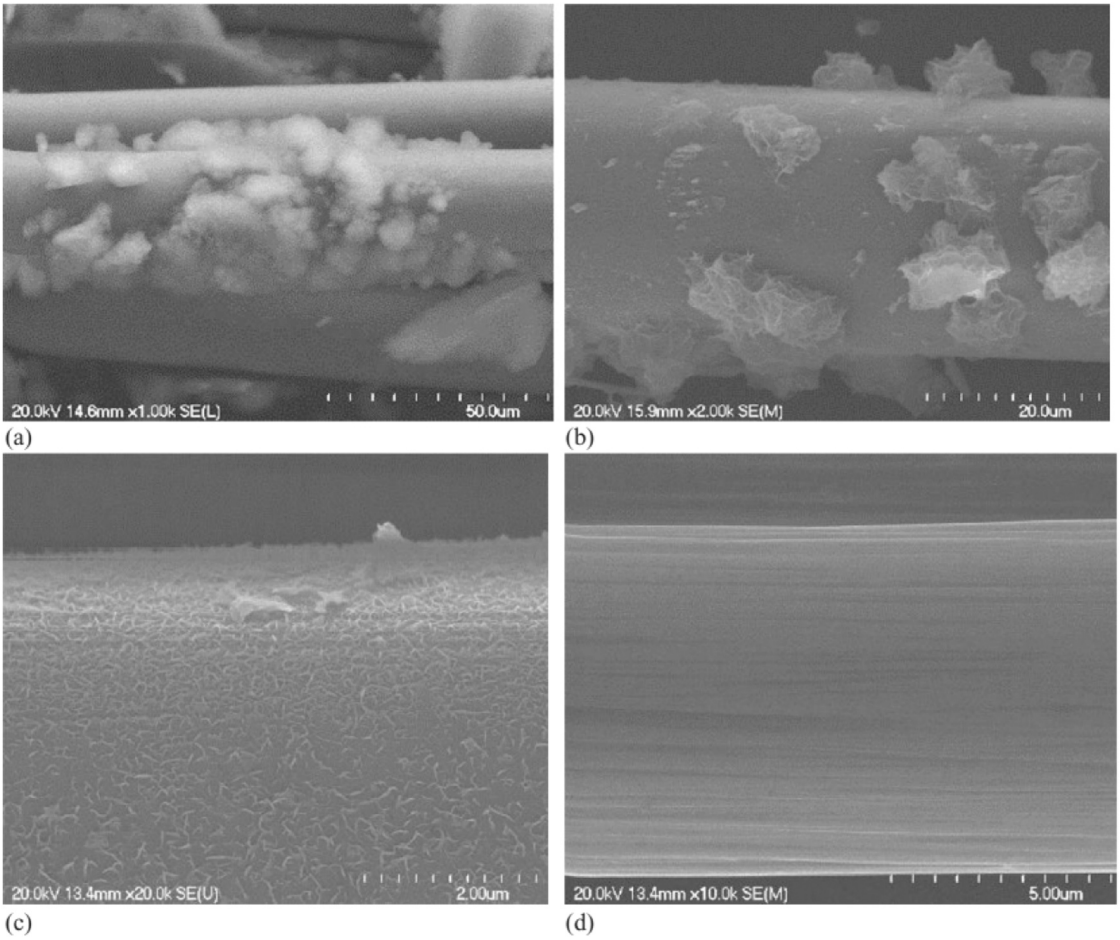

Fig. 7. SEM images showing four types of fibre surfaces after conditioning: (a) E-glass fibre; (b) ECR-glass fibre; (c) basalt fibre; and (d) carbon fibre [27].

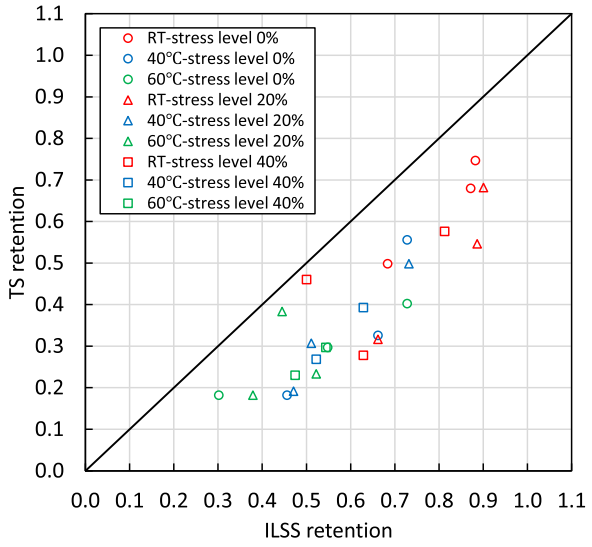

Fig. 8. Effect of sustained stress on relationship between TS and ILSS retentions of GFRP bars.

beam specimens were immersed in seawater up to 270 days at 20℃ with sustained load levels of 25 % and 40 % of the ultimate load. They conducted SEM analysis after conditioning as shown in Fig. 9. The SEM revealed that after 270 days of the combined influence of seawater exposure and sustained load, the corrosion depth along the radial direction of the bar extended, and the area of the void caused by debonding increased. Won et al. [61] examined the degradation of GFRP bars made from E-glass fibres and vinyl-ester resin in an alkaline solution up to 300 days at 20, 40, 60, and 80℃. It was shown that TS retention had a high correlation with total volume of pores in the GFRP bars. When immersed in an alkaline solution for over 90 days, the pores increased dramatically, which reflects the increased delamination and cracks in the polymer matrix of the GFRP bars. Park et al. [62] investigated the degradation of GFRP dowel bars made of E-glass fibres and vinyl-ester resin in an alkaline solution up to 80 days at 20℃. They showed that as total volume of pores in the bars increased, the ILSS decreased with immersion days. It can be therefore inferred that voids caused by debonding in GFRP bars due to the combination of alkaline conditioning and sustained stress can lead to a reduction in both TS and ILSS, and then the relationship between TS and ILSS can be maintained.

The stress of GFRP bars as internal reinforcement in concrete structures is designed to be suppressed to avoid creep-rupture as serviceability requirements. At the time of construction of the bridge barrier and bridge deck infrastructure reported in Table 2, the ACI

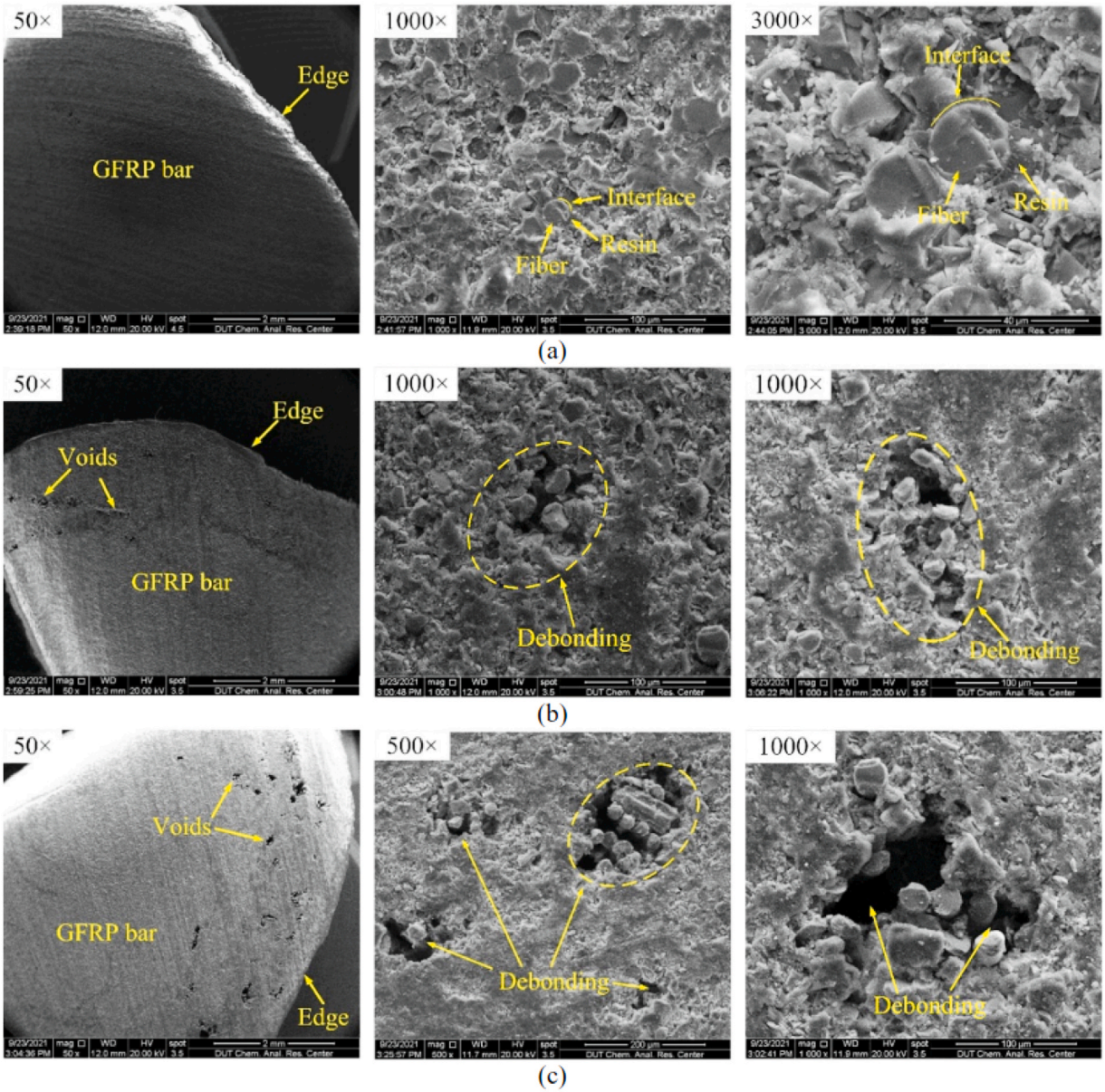

Fig. 9. SEM images showing the degradation in fibre-resin interface with sustained load: (a) unconditioned sample; (b) sample after seawater exposure; and (c) sample with 40 % sustained load level after seawater exposure [60].

design code recommended that service-load sustained stress should not exceed 0.20 times the design tensile strength f_{fu} of GFRP reinforcement, where f_{fu} is equal to the guaranteed tensile strength multiplied by an environmental reduction factor [63]. Whereas the current ACI design code [64] shows the limit for a safe sustained stress level is set at 0.30 f_{fu}. Therefore, it may be concluded that the relationship described in Fig. 2 can also be applicable to GFRP bars in concrete structures subjected to sustained stress.

3.3. Summary and future research

The analyses and discussion of the test data shows that there is a relationship between TS and ILSS of vinyl-ester based GFRP bars. The relationship can be maintained as the condition period increases and be subjected to sustained stress. However, it is also shown that the reduction rate of ILSS cannot be determined by only the types of glass fibres or types of the resin system. This result suggests that the relationship between TS and ILSS retentions should be assessed before the structure is operational in order to reliably correlate the retention of ILSS with that of TS and to be used as an indicator of the in-service durability of GFRP bars. The next section shows a comparison of the ILSS retention of vinyl-ester based GFRP bars exposed in the field with the predicted results, based on the fact that the relationship between TS and ILSS has been confirmed.

For future research, it would be useful to model the prediction of TS and ILSS, by focusing on the damaged area and on the damaged component of the fibre, the resin and the fibre/resin interface, as shown in Fig. 6. For example, Zhao et al. [65] developed a chemical etching-based model and a hydroxyl ion diffusion-based model for to predict TS, which are based on the damage area of the bars. A similar development may lead to a quantitative assessment of the relationship between TS and ILSS.

4. Prediction of field durability of GFRP bars based on ILSS

4.1. Prediction method

Manalo et al. [46] conducted a comprehensive experiment on the ILSS of vinyl-ester based GFRP bars (nominal diameter of 9.53 mm, fibre content: 80.9 wt%) in an alkaline environment. The experiment had immersion tests in tap water (TW), saline solution (SS) and alkaline solution (AS) using bare bars and concrete-embedded bars (a cover of 7.5 mm) with different exposure durations (28, 56, and 112 days) and at various temperatures (23, 60, 80℃). The concrete had a water-to-cement ratio of 0.45, and the pH of the hardened cement paste was 12.8. It was revealed that the ILSS retention of the concrete-embedded GFRP bars is generally higher than that of the bare GFRP bars under similar immersion conditions. This result can be attributed to the presence of the concrete cover which limited the availability of moisture around the bars since the rate of degradation of GFRP bars exposed to fluid environments is related to the rate of fluid sorption [44]. Based on the ILSS retention of the concrete-embedded GFRP bars, master curves to predict the long-term behaviour were constructed, using a logarithmic equation with the Arrhenius model to express the degradation rate for materials with time. The master curve of ILSS retention of each immersion solution considering the time-shift factor (TSF) is given by Eq. 1.

$$ILSS\ retention(\%) = a\ln(t \bullet TSF) + b \tag{1}$$

where a and b are regression constants, t is time in day or year, and TSF is given by Eq. 2.

$$TSF = \exp\left[\frac{E_a}{R}\left(\frac{1}{T_{ref}} - \frac{1}{T_0}\right)\right] \tag{2}$$

where E_a/R is the regression constant in the Arrhenius-plot, T_{ref} and T_0 are the reference and exposure temperatures. These values are summarized in Table 3. The regression constants were derived from all the data of the time required to reach a specific strength retention corresponding to its TSF, considering the effect of temperature.

For comparison, a prediction model of the ILSS retention of epoxy-based GFRP bars (nominal diameter of 6 mm, fibre content: 62.8 vol%) by Wang et al. [45] is also used, which was developed based on the results of bare bars conditioned in alkaline solution at pH of 13.4. The ILSS was determined in accordance with ASTM D 4475 [31], which had a horizontal shear failure mode. As the model uses an exponential model with the Arrhenius model, it can account for the TSF as mentioned above. Note that the bare bars showed higher ILSS retention than those of Manalo et al. [46].

Table 3
Regression constants and TSF for prediction.

Immersion agent	Regression constants				*TSF*				
	a	b (for time in day)	b (for time in year)	E_a/R	4℃	11℃	14℃	23℃	26℃
TW	−3.550	108.5	87.6	8946	0.126	0.279	0.387	1.000	1.351
SS	−3.725	109.0	87.0	4599	0.344	0.518	0.614	1.000	1.167
AS	−4.569	102.1	75.1	4642	0.341	0.515	0.611	1.000	1.169

4.2. Results and discussion

Fig. 10 shows the actual test set-up of the laboratory experiment described in Section 4.1 and the failure mode of the conditioned specimens. The short-beam shear test was performed on GFRP bars (nominal diameter of 9.53 mm) with a clear span of three-times the bar diameter and an overhang length of 0.5-times the bar diameter. The interlaminar shear test was performed using an MTS 100 kN testing machine at a controlled displacement rate of 1.3 mm/min at 23 ± 2°C and 50 ± 5 % relative humidity. It was reported that all the specimens failed due to horizontal shear originating at the edge of the bars and developing along bar length [46]. Fig. 11 shows images of GFRP bars extracted from the bridge barrier, bridge decks, and exposed specimens and the failure mode of the specimen extracted from the bridge barrier. No visual damage was reported in the extracted specimens shown in Fig. 11 (a), (b), (c) [28,30,33]. The failure mode of the field data shown in Table 2 is consistent with the exception of Study No.2.

Fig. 12 shows a comparison of ILSS retention with time between field exposure data and predicted results up to 100 years. The predicted results were calculated by considering the annual mean temperature of each place as shown in Table 2. Summarising the predicted results, ILSS retentions exposed to TW, SS and AS can reach 70 %-79 %, 69 %-74 % and 53 %-59 %, respectively after 100 years of service. It can be noted that as the annual mean temperature increases, the predicted results of TW and SS become closer as shown in Fig. 12. The predicted results of Wang et al. [45] show that the model based on bare bars conditioned in alkaline solution can give conservative results, especially at higher temperatures.

In Fig. 12 (a), the field exposure data shows 86 % ILSS retention, and this agrees well with the predicted result obtained from the immersion test by TW. Benmokrane et al. [28] reported that in the bridge barrier, the moisture content of the concrete surrounding the GFRP bars was kept high, and relative humidity was always more than 80 %. It is thought that the environment surrounding the bars in the bridge wall was close to that in the immersion test by TW. In Fig. 12 (b), the field exposure data shows 73 % of ILSS retention, and this result is plotted almost at the midpoint of the predicted results of SS and AS. AI-Khafaji et al. [30] reported that the GFRP bars in Fig. 12 (b) had a relatively high-water absorption, more than 1 % at equilibrium, as measured by ASTM D570 [66]. This result is consistent with that of Yu et al. [44] in which higher water absorption resulted in a greater reduction in ILSS of GFRP bars. Another possible reason for the difference in results shown in Fig. 12 (a) could be a transverse cracking [11] in the bridge deck which can accelerate deterioration due to freeze-thaw cycles of water in cracks and water leakage [67]. Yang et al. [68] observed the presence of damage in the concrete specimens exposed to freezing and thawing cycles increased both the initial sorptivity and total water absorption of the concrete specimens. Shin et al. [69] conducted a water permeability test on concrete specimens with crack widths of 0.1–0.5 mm and showed that the water flow rate increased with increasing crack width. Therefore, the existing concrete crack could also lead to the environment surrounding the bars in the bridge deck being subjected to more moisture where ILSS retention can be further lower [46]. In Fig. 12 (c), the field exposure data shows 76 % and 93 % of ILSS retention. Even in the same bridge deck, a 17 % difference is observed. This could be attributed to a different water content in concrete pores since the lower water content in concrete pores related to relative humidity leads to the lower degradation of GFRP bars [70]. In Fig. 12 (d), the field exposure data shows 71 % of ILSS retention, which is lower than the predicted results of TW and SS. In a similar result to Fig. 12 (b), Ramanathan et al. [52] reported that the GFRP bars in Fig. 12 (d) had a relatively high-water absorption, greater than 1 % at equilibrium, as measured by ASTM D570 [66]. The different failure mode described in Section 2.2 could result in a lower ILSS retention. In Fig. 12 (e), the field exposure data obtained from a tidal zone shows 78 % and 84 % of ILSS retention, these results are higher than the predicted results of TW and SS. This result is consistent with that of Almusallam [71] in which GFRP bars (12 mm diameter) were embedded in concrete with a 19 mm cover and tested with immersion to TW or dry and wet cycle to seawater at 50℃. Chrisp et al. [72] studied cover-zone concrete under a cyclic wetting and drying regime to TW and SS by using in situ electrical measurements. It was shown that the wetting and drying regime applied to the concrete surface caused a marked response at the electrodes positioned at 5 mm to 30 mm while it did not occur at 50 mm, meaning that water content in concrete pores was kept high during the cycles. Therefore, it can be inferred that the concrete cover (25 mm) surrounding the GFRP bars had a relatively low water content due to the wet and dry cycles during the exposure test.

In summary, the field exposure results were close to the predicted results of TW or SS, while the predicted results of AS are

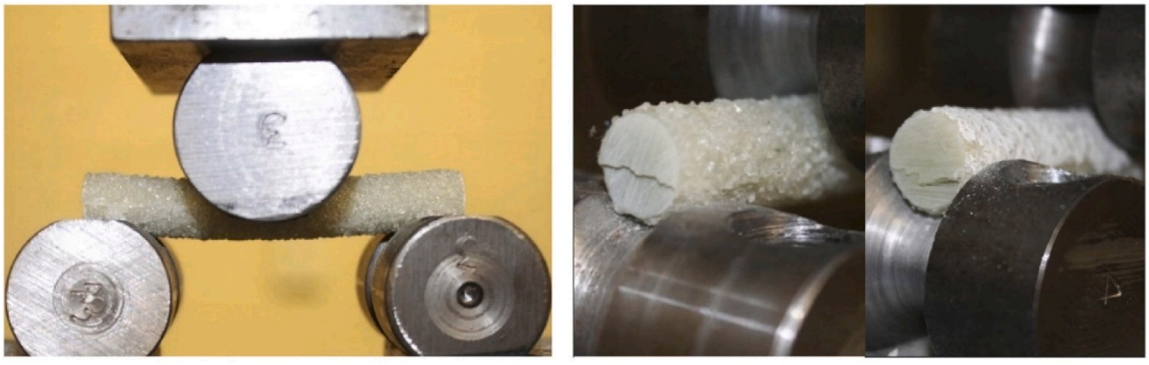

Fig. 10. Test setup and failure mode of laboratory specimens [46].

(a) Extracted specimens from bridge decks: left: Ohio; right: Texas [30]

(b) Extracted GFRP bars from exposure test specimens [33]

(c) Extracted GFRP bars from the bridge barrier [28]

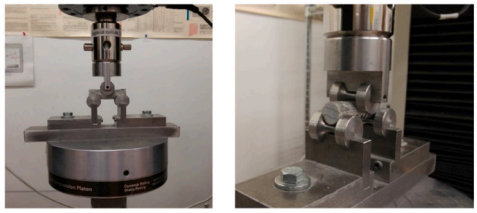

(d) Test setup and failure mode of extracted GFRP bars from the bridge barrier [28]

Fig. 11. Extracted specimens from field exposure, test setup, and failure modes.

considered conservative. It is thought that hardened concrete in the field is not subjected to the continuous exposure of alkaline as much as the immersion to AS while it is subjected to the moisture from rainfall and snowfall and chloride from deicing salt or seawater. Bérube et al. [73] investigated chloride and sodium profiles in concrete cores extracted from nine bridges in Québec, Canada to determine whether or not they were subjected to deicing salts. They revealed that sodium and OH^- ion contents tended to be a low level to those bridges that had not been exposed to deicing salts while the chloride profile showed high contents near the surface and decreased with depth. It was therefore suggested that exposure to deicing salts (NaCl) does not increase the OH^- ion and the pH in the concrete pore solution, which affects the durability of GFRP bars [23]. Thus, it can be noted that concrete-embedded GFRP bars immersed to AS are subjected to a more severe environment than that of a field environment. For future verification with field data, it is recommended that water content in concrete and water absorption of GFRP bars should be obtained as well as ILSS since they were key properties that will help explain the mechanism that affects the long-term performance of the bars.

As ASTM D7957/D7957M [57], the standard specification for GFRP bars requires alkaline resistance for 80 % of TS retention following 90 days at 60℃, time to reach 80 % of ILSS retention is estimated using the master curves for TW and SS which agree well with the field exposure results. Fig. 13 shows the relationship between time to reach 80 % of ILSS retention and temperature from 23℃ to 80℃. For TW and SS at 60℃, 108 days and 430 days are needed to reach 80 % of ILSS retention, respectively. Based on the result of TW at 60℃, the acceleration rates to field exposure at the annual temperatures 4℃, 11℃, 14℃, and 26℃ shown in Fig. 12 are obtained as 227, 103, 74, and 26 times, respectively. Meanwhile, at higher temperatures, the time to reach 80 % of ILSS retention of TW is much faster than that of SS. This may be due to the higher moisture uptake of the GFRP bars in TW than in SS. Manalo et al. [46] showed that

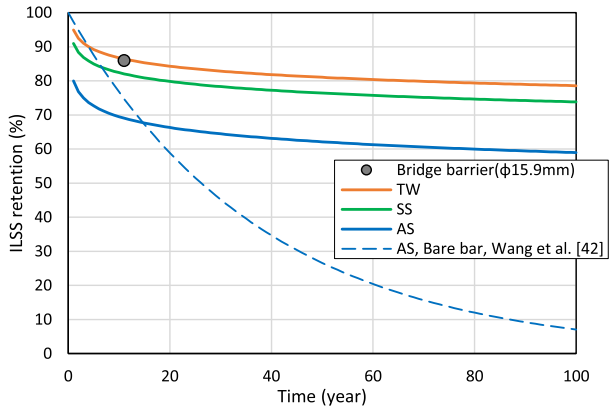

(a) Bridge barrier in Quebec, Canada (4.0°C)

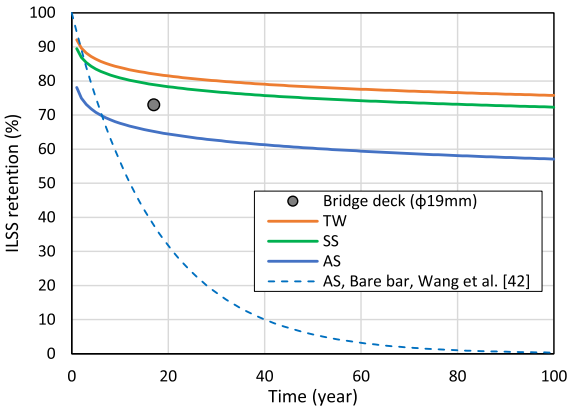

(b) Bridge deck in Ohio, United States (11°C)

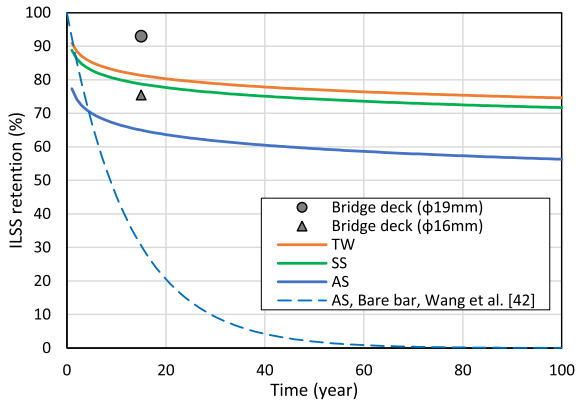

(c) Bridge deck in Texas, United States (14°C)

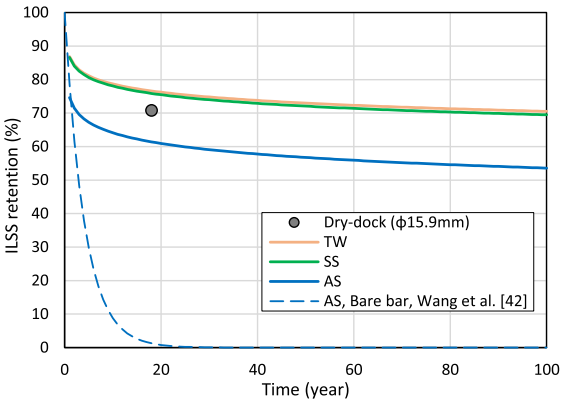

(d) Dry deck in Hawaii, United States (25°C)

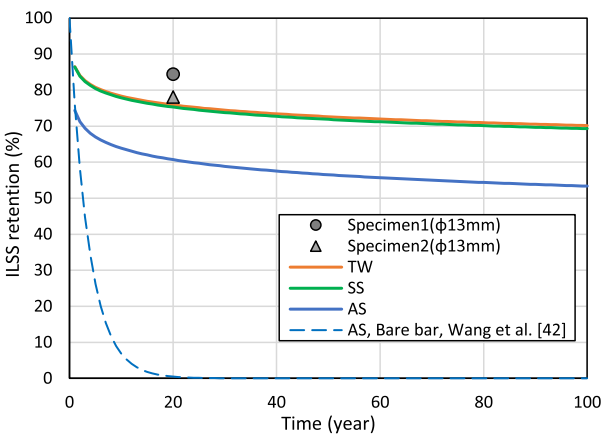

(e) Exposure specimens in Jubail, Saudi Arabia (26°C)

Fig. 12. Comparison of ILSS retention with time between field exposure data and predicted results based on concrete-embedded GFRP bars up to 100 years (the annual mean temperature of each place is provided in parentheses).

the diffusion rate of the GFRP bars exposed in TW was higher than that in SS. This could also be explained by the higher water activity of TW compared to SS, which leads to a higher osmotic pressure and therefore higher moisture uptake at interfaces [74].

This information can help to assess the field durability of GFRP bars based on ILSS by laboratory tests. Moreover, the results of the comparison and analysis of the extensive data obtained from the laboratory experiments and those from field-exposed actual structures suggest that the simpler ILSS tests can be considered as an alternative to the complex and time-consuming tensile test suggested by the

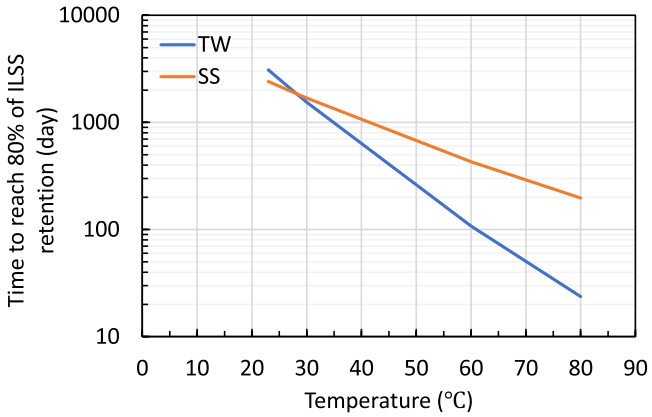

Fig. 13. Relationship between time to reach 80 % of ILSS retention and temperature.

ASTM D7957/D7957M [57] for evaluating the durability of GFRP bars.

5. Conclusions

This study conducted an intensive review and analysis on the relationship of the durability of vinyl-ester based GFRP bars between tensile strength (TS) and interlaminar shear strength (ILSS), which were obtained from laboratory experiments and field exposure tests. A summary of the experimental database of 11- to 20-year-old GFRP bars in field exposure, where ILSS retentions are available, was described, and then results of field investigations and long-term predictions were compared. The following conclusions can be drawn from this study:

- There is a high correlation between the TS and ILSS retentions of GFRP bars after alkaline conditioning from laboratory experiments. TS and ILSS retentions showed 0.18–0.92 and 0.30–0.92, respectively. Microscopic observation revealed damage to the fibre, resin, and fibre-resin interface near the exposed surface.
- For some of the GFRP bars, the reduction of ILSS is much slower than that of TS. In this case, TS retention was 0.65–0.97 while ILSS retention remained from 0.88 to 1.0. Microscopic observation revealed damage to the fibre-resin interface near the exposed surface. The GFRP bars showing a much slower reduction in ILSS cannot be specified by only the types of glass fibres or resin systems.
- The relationship between TS and ILSS of GFRP bars can be almost the same with/without sustained stress. Microscopic observation revealed that voids caused by debonding in GFRP bars were due to the combination of alkaline conditioning and sustained stress.
- By validating the field exposure data from the four structures and from the one exposure test with ILSS retention ranging from 0.71 to 0.93, the ILSS of GFRP bars extracted from field exposed structures results showed a very good correlation to the predicted ILSS of concrete embedded GFRP bars exposed in tap water or saline solution, while the predicted results of alkaline solution were considered conservative.

The above results showed a high correlation between TS and ILSS of vinyl-ester based GFRP bars from the extensive data obtained from laboratory experiments and those from field exposed actual structures. This suggests that the simpler ILSS tests can be considered as an alternative to the tensile test suggested by the ASTM D7957/D7957M [57] for evaluating the durability of GFRP bars. Moreover, it is recommended that water content of concrete and water absorption of GFRP bars in the field should be obtained as well as ILSS since they were key properties that will help evaluate the long-term performance of the bars.

CRediT authorship contribution statement

Manalo Allan: Writing – review & editing, Supervision, Resources, Project administration, Methodology, Funding acquisition, Conceptualization. **Sakuraba Hiroki:** Writing – review & editing, Writing – original draft, Validation, Methodology, Funding acquisition, Formal analysis, Data curation, Conceptualization. **Benmokrane Brahim:** Writing – review & editing, Supervision, Funding acquisition. **Alajarmeh Omar:** Writing – review & editing, Supervision, Conceptualization.

Declaration of Competing Interest

The authors declare that they have no known competing financial interests or personal relationships that could have appeared to influence the work reported in this paper.

Acknowledgements

The authors acknowledge the financial support from the Cooperative Research Centre Project (CRCPXIII000007), the ARC Discovery Project (DP230101152) on Degradation mechanisms of structural composites under extreme weather, and the Natural Science and Engineering Research Council (NSERC) of Canada. The first author gratefully acknowledges the financial support provided by the visiting research program between the University of Southern Queensland, Australia and the Public Works Research Institute, Japan.

Data Availability

Data will be made available on request.

References

[1] S.D. Cramer, B.S. Covino Jr., S.J. Bullard, G.R. Holcomb, J.H. Russell, F.J. Nelson, H.M. Laylor, S.M. Soltesz, Corrosion prevention and remediation strategies for reinforced concrete coastal bridges, Cem. Concr. Compos 24 (2002) 101–117.
[2] H. Tatematsu, T. Sasaki, Repair materials system for chloride-induced corrosion of reinforcing bars, Cem. Concr. Compos 25 (2003) 123–129.
[3] Francesca Ceroni, Edoardo Cosenza, Manfredi Gaetano, Marisa Pecce, Durability issues of FRP rebars in reinforced concrete members, Cem. Concr. Compos 28 (2006) 857–868.
[4] A.C. Manalo, P. Mendis, Y. Bai, B. Jachmann, C.D. Sorbello, Fiber-reinforced polymer bars for concrete structures: state-of-the-practice in Australia, J. Compos. Constr. (2020).
[5] Julio F. Davalos, Yi Chen, Indrajit Ray, Effect of FRP bar degradation on interface bond with high strength concrete, Cem. Concr. Compos 30 (2008) 722–730.
[6] Mathieu Robert, Brahim Benmokrane, Effect of aging on bond of GFRP bars embedded in concrete, Cem. Concr. Compos 30 (2010) 461–467.
[7] Saleh Hamed Alsayed, Flexural behaviour of concrete beams reinforced with GFRP bars, Cem. Concr. Compos 20 (1998) 1–11.
[8] Kader Laoubi, Ehab El-Salakawy, Brahim Benmokrane, Creep and durability of sand-coated glass FRP bars in concrete elements under freeze/thaw cycling and sustained loads, Cem. Concr. Compos 28 (2006) 869–878.
[9] G.B. Maranan, A.C. Manalo, B. Benmokrane, W. Karunasena, P. Mendis, Evaluation of the flexural strength and serviceability of geopolymer concrete beams reinforced with glass-fibre-reinforced polymer (GFRP) bars, Eng. Struct. 101 (2015) 529–541.
[10] Chad Klowak, Amjad Memon, Aftab Mufti, Static and fatigue investigation of second generation steel-free bridge decks, Cem. Concr. Compos 28 (2006) 890–897.
[11] Amir Ghatefar, Ehab El-Salakawy, M.T. Bassuoni, Early-age restrained shrinkage cracking of GFRP-RC bridge deck slabs: effect of environmental conditions, Cem. Concr. Compos 64 (2015) 62–73.
[12] Mohammed Al-Rubaye, Allan Manalo, Omar Alajarmeh, Wahid Ferdous, Weena Lokuge, Brahim Benmokrane, Azam Edoo, Flexural behaviour of concrete slabs reinforced with GFRP bars and hollow composite reinforcing systems, Compos. Struct. 236 (2020) 111836.
[13] O.S. AlAjarmeh, A.C. Manalo, B. Benmokrane, W. Karunasena, P. Mendis, K.T.Q. Nguyen, Compressive behavior of axially loaded circular hollow concrete columns reinforced with GFRP bars and spirals, Constr. Build. Mater. 194 (2019) 12–23.
[14] JinJing Liao, Bo Di, Yu Zheng, Zhi-Wen Xuan, Jun-Jie Zeng, Shear behavior of circular concrete short columns reinforced with GFRP longitudinal bars and CFRP grid stirrups, Compos. Struct. 340 (2024) 118181.
[15] Simone Spagnuolo, Alberto Meda, Zila Rinaldi, Antonio Nanni, Precast Concrete Tunnel Segments with GFRP Reinforcement, J. Compos. Constr. 21 (5) (2017) 04017020.
[16] Brahim Benmokrane, Ehab El-Salakawy, Sherif El-Gamal, Sylvain Goulet, Construction and testing of an innovative concrete bridge deck totally reinforced with glass FRP bars: Val-Alain Bridge on highway 20 east, J. Bridge Eng. 12 (5) (2007) 632–645.
[17] Allan Manalo, Omar Alajarmeh, Xian Yang, Wahid Ferdous, Shahrad Ebrahimzadeh, Brahim Benmokrane, Charles-Dean Sorbello, Senarath Weerakoon, Darren Lutze, Development and mechanical performance evaluation of a GFRP-reinforced concrete boat-approach slab, Struct 46 (2022) 73–87.
[18] Brahim Benmokrane, Salaheldin Mousa, Khaled Mohamed, Mahmoud Sayed-Ahmed, Physical, mechanical, and durability characteristics of newly developed thermoplastic GFRP bars for reinforcing concrete structures, Constr. Build. Mater. 276 (2021) 122200.
[19] Jun-Jie Zeng, Zhi-Hao Hao, Yuan-Yuan Jiang, Qi-Jin Liang, Yue Liu, Yan Zhuge, Long-term durability of UHPECC-embedded GFRP bars in alkaline environments, J. Compos. Constr. 28 (6) (2024) 04024065.
[20] Jun-Jie Zeng, Zhi-Hao Hao, Hou-Qi Sun, Wei-Bin Zeng, Tian-Hui Fan, Yan Zhuge, Durability assessment of ultra-high-performance concrete (UHPC) and FRP grid-reinforced UHPC plates under marine environments, Eng. Struct. 323 (2025) 119313.
[21] JinJing Liao, Yu Zheng, Haotian Li, Yong Yu, Yingwu Zhou, Tension stiffening and cracking behavior of FRP-reinforced self-compacting concrete with high-volume fly ash (HVFA-SCC), Constr. Build. Mater. 456 (2024) 139219.
[22] JinJing Liao, Jun-Jie Zeng, Yu-Lei Bai, Lihai Zhang, Bond strength of GFRP bars to high strength and ultra-high strength fiber reinforced seawater sea-sand concrete (SSC), Compos. Struct. 281 (2022) 115013.
[23] Yi Chen, Julio F. Davalos, Indrajit Ray, Durability prediction for GFRP reinforcing bars using shot-term data of accelerated aging tests, J. Compos. Constr. (2006).
[24] Mathieu Robert, Patrice Cousin, and Brahim Benmokrane, Durability of GFRP Reinforcing Bars Embedded in Moist Concrete, J. Compos. Constr., 10.1061/(ASCE)1090-0268, 2009, 13:2, 66.
[25] Mathieu Robert, Brahim Benmokrane, Combined effects of saline solution and moist concrete on long-term durability of GFRP reinforcing bars, Constr. Build. Mater. 38 (2013) 274–284.
[26] Jia-Hui Sun, Nian-Jiu Su, Zhou-Qiong He, Rui-Xin Jia, Yue Liu, Fu-Kuan Lin, Thierno Aliou Ka, Durability of concrete-encapsulated GFRP bars subjected to seawater immersion, Case Stud. Constr. Mater. 20 (2024) e03249.
[27] B. Benmokrane, M. Hassan, M. Robert, P.V. Vijay, A. Manalo, Effect of different constituent fiber, resin, and sizing combinations on alkaline resistance of basalt, carbon, and glass FRP bars, J. Compos. Constr. (2020).
[28] Brahim Benmokrane, Claude Nazair, Marc-Antoine Loranger, Allan Manalo, Field durability study of vinyl-ester-based GFRP rebars in concrete bridge barriers, J. Bridge Eng. (2018).
[29] Vanessa Benzecry, Ali F. Al-Khafaji, Rudy T. Haluza, Charles E. Bakis, Jhon J. Myers and Antonio Nanni, Durability assessment of 15- to 20-year-old GFRP bars extracted from bridges in the US I: Selected bridges, bar extraction, and concrete assessment, J. Compos. Constr., 2021.
[30] Ali F. Al-Khafaji, Rudy T. Haluza, Vanessa Benzecry, Jhon J. Myers, Charles E. Bakis, Antonio Nanni, Durability assessment of 15- to 20-year-old GFRP bars extracted from bridges in the US II: GFRP bar assessment, J. Compos. Constr. (2021).
[31] ASTM Standard ASTM D4475, Standard test method for apparent horizontal shear strength of pultruded reinforced plastic rods by the short-beam method, ASTM D4475-21, ASTM International, West Conshohocken, Pa, 2021.
[32] ASTM Standard ASTM D7205/D7205M, Standard Test Method for Tensile Properties of Fiber Reinforced Polymer Matrix Composite Bars, ASTM D7205/D7205M-21, ASTM International, West Conshohocken, Pa, 2021.
[33] M. Mesfer, Al-Zahrani, Durability of concrete-embedded GFRP bars after 20 years of tidal zone exposure: correlation with accelerated aging tests, Case Stud. Constr. Mater. 21 (2024) e03435.
[34] Francesco Micelli, Antonio Nanni, Durability of FRP rods for concrete structures, Constr. Build. Mater. 18 (2004) 491–503.

[35] Hyeong-Yeol Kim, Young-Hwan Park, Young-Jun You, Chang-Kwon Moon, Short-term durability test for GFRP rods under various environmental conditions, Compos. Struct. 83 (2008) 37–47.
[36] Brahim Benmokrane, Allan Manalo, Jean-Charles Bouhet, Khaled Mohamed, Mathieu Robert, Effects of diameter on the durability of glass fiber–reinforced polymer bars conditioned in alkaline solution, J. Compos. Constr. (2017).
[37] Matteo Di. Benedetti Hamed Fergani, Cyril Lynsdale Cristina Miàs Oller, Maurizio Guadagnini, Durability and degradation mechanisms of GFRP reinforcement subjected to severe environments and sustained stress, Constr. Build. Mater. 170 (2018) 637–648.
[38] Ahmed H. Ali, Hamdy M. Mohamed, Brahim Benmokrane, Bar size effect on long-term durability of sand-coated basalt-FRP composite bars, Compos. Part B (2020) 108059.
[39] Carlos N. Morales, Guillermo Claure, Alvaro Ruiz Emparanza, Antonio Nanni, Durability of GFRP reinforcing bars in seawater concrete, Constr. Build. Mater. 270 (2021) 121492.
[40] Zhongyu Lu, Shixin Li, Jianhe Xie, Quanmeng Huang, Baifa Zhang, Peiyan Huang, Jianglin Li, Lijuan Li, Durability of GFRP bars embedded in seawater sea-sand concrete: a coupling effect of prestress and immersion in seawater, Constr. Build. Mater. 326 (2022) 126979.
[41] Noémie Delaplanque, Maxime Tharreau, Sylvain Chataigner, Marc Quiertant, Karim Benzarti, Ludwig Battais, Arnaud Rolland, Laurent Gaillet, Xavier Bourbon, Durability of partially cured GFRP reinforcing bars in alkaline environments with or without sustained tensile load, Constr. Build. Mater. 442 (2024) 137603.
[42] Guangyan Feng, Shuaicheng Guo, Linlin Zhou, Wenheng Luo, Xiangke Guo, Zuquan Jin, Deju Zhu, Effects of surface characteristics and alkalinity on the deterioration of BFRP bars and BFRP-SSC interface in seawater environment, Compos. Part B 268 (2024) 111072.
[43] Xiangke Guo, Zuquan Jin, Chuansheng Xiong, Bo Pang, Dongshuai Hou, Weihua, Degradation of mechanical properties and microstructure evolution of basalt-carbon based hybrid FRP bars in real seawater and sea-sand concrete, Compos. Part B 271 (2024) 111163.
[44] Yixun Yu, Shuai Liu, Yunfeng Pan, Xinbo Miu, Jintao Liu, Durability of glass fiber-reinforced polymer bars in water and simulated concrete pore solution, Constr. Build. Mater. 299 (2021) 123995.
[45] Zike Wang, Xiao-Ling Zhao, Guijun Xian, Gang Wu, R.K. Singh Raman, Saad Al-Saadi, Durability study on interlaminar shear behaviour of basalt-, glass- and carbon-fibre reinforced polymer (B/G/CFRP) bars in seawater sea sand concrete environment, Constr. Build. Mater. 156 (2017) 985–1004.
[46] Allan Manalo, Ginghis Maranan, Brahim Benmokrane, Patrice Cousin, Omar Alajarmeh, Wahid Ferdous, Ray Liang, Gangarao Hota, Comparative durability of GFRP composite reinforcing bars in concrete and in simulated concrete environments, Cem. Concr. Compos 109 (2020) 103564.
[47] Guangyan Feng, Deju Zhu, Shuaicheng Guo, Md Zillur Rahman, Zuquan Jin, Caijun Shi, A review on mechanical properties and deterioration mechanisms of FRP bars under severe environmental and loading conditions, Cem. Concr. Compos 134 (2022) 104758.
[48] Weiwei Wu, Xiongjun He, Wenrui Yang, Li Dai, Yingang Wang, Jia He, Long-time durability of GFRP bars in the alkaline concrete environment for eight years, Constr. Build. Mater. 314 (2022) 125573.
[49] Jun-Jie Zeng, Zhi-Hao Hao, Qi-Jin Liang, Yan Zhuge, Yue Liu, Durability assessment of GFRP bars exposed to combined accelerated aging in alkaline solution and a constant load, Eng. Struct. 297 (2023) 116990. Zhi-Hao.
[50] Jie-Kai Zhou, Zhi-Hao Hao, Jun-Jie Zeng, Sheng-Zhao Feng, Qi-Jin Liang, Bin Zhao, Ran Feng, Yan Zhuge, Durability assessment of GFRP bars embedded in UHP-ECCs subjected to an accelerated aging environment with sustained loading, Constr. Build. Mater. 419 (2024) 135364.
[51] ASTM Standard ASTM D3916, Standard Test Method for Tensile Properties of Pultruded Glass-Fiber-Reinforced Plastic Rod, ASTM D3916-22. West Conshohocken, ASTM International, West Conshohocken, Pa, 2022.
[52] Sivakumar Ramanathan, Vanessa Benzecry, Prannoy Suraneni, Antonio Nanni, Condition assessment of concrete and glass fiber reinforced polymer (GFRP) rebar after 18 years of service life, Case Stud. Constr. Mater. 14 (2021) e00494.
[53] Omid Gooranorimi, Antonio Nanni, GFRP reinforcement in concrete after 15 years of service, J. Compos. Constr. (2017) 04017024.
[54] Brahim Benmokrane, Fareed Elgabbas, Ehab A. Ahmed, Patrice Cousin, Characterization and comparative durability study of glass/vinylester, basalt/vinylester and basalt/epoxy FRP bars, J. Compos. Constr. 19 (6) (2015) 04015008.
[55] Tuanjie Wang, Abdul Ghani Razaqpur, Shaoliang Chen, Durability of GFRP and BFRP reinforcing bars in simulated seawater sea sand calcium sulfoaluminate cement concrete pore solution, J. Build. Eng. 80 (2023) 107954.
[56] Zenon Achillides, Kypros Pilakoutas, Bond behavior of fiber reinforced polymer bars under direct pullout conditions, J. Compos. Constr. 8 (2) (2004).
[57] ASTM Standard ASTM D7957, Standard Specification for Solid Round Glass Fiber Reinforced Polymer Bars for Concrete Reinforcement. ASTM D7957-22, ASTM International, West Conshohocken, Pa, 2022.
[58] Gilbert Nkurunziza, Ahmed Debaiky, Patrice Cousin, Brahim Benmokrane, Durability of GFRP bars: a critical review of the literature, Prog. Struct. Eng. Mater. 7 (2005) 194–209.
[59] Brahim Benmokrane, Peng Wang, Tan Minh Ton-That, Habib Rahman, Jean-Francois Robert, Durability of glass fiber-reinforced polymer reinforcing bars in concrete environment, J. Compos. Constr. 6 (3) (2002) 143–153.
[60] Yufei Chang, Yanlei Wang, Bingnan Li, Mifeng Wang, Zhi Zhou, Jinping Ou, GFRP bar-reinforced seawater sea-sand concrete beam under the combined influence of seawater exposure and sustained load: durability and degradation mechanism, Structures 43 (2022) 1503–1515.
[61] Jong-Pil Won, Su-Jin Lee, Yoon-Jung Kim, Chang-Il Jang, Sang-Woo Lee, The effect of exposure to alkaline solution and water on the strength–porosity relationship of GFRP rebar, Compos. Part B 39 (2008) 764–772.
[62] Chan-Gi Park, Chang-Il Jang, Si-Won Lee, Jong-Pil Won, Microstructural investigation of long-term degradation mechanisms in GFRP dowel bars for jointed concrete pavement, J. Appl. Polym. Sci. 108 (2008) 3128–3137.
[63] Brahim Benmokrane, Vicki L. Brown, Khaled Mohamed, Antonio Nanni, Marco Rossini, Carol Shield, Creep-rupture limit for GFRP bars subjected to sustained loads, Vol.6, No.3, J. Compos. Constr. 23 (6) (2019) 06019001.
[64] ACI (American Concrete Institute), Specification for Carbon and Glass Fiber-reinforced Polymer Bar Materials for Concrete Reinforcement, in: ACI, 440, ACI, Farmington Hills, MI, 2022, pp. 11–22.
[65] Qi Zhao, Xiao-Ling Zhao, Daxu Zhang, Jian-Guo Dai, Xuanyi Xue, Degradation of GFRP bars with epoxy and vinyl ester matrices in a marine concrete environment: an experimental study and theoretical modeling, J. Compos. Constr. 28 (2) (2024) 04024004.
[66] ASTM, Standard ASTM D570 Water Absorption of Plastics, ASTM D570-22, ASTM International, West Conshohocken, Pa, 2022.
[67] Rambod Hadidi, Ala Saadeghvaziri, Transverse cracking of concrete bridge decks: state-of-the-art, J. Bridge Eng. 10 (5) (2005).
[68] Zhifu Yang, W. Jason Weiss, Jan Olek, Water transport in concrete damaged by tensile loading and freeze-thaw cycling, J. Mater. Civ. Eng. 18 (3) (2006).
[69] Kyung Joon Shin, Wonho Bae, Seul-Woo Choi, Min Woo Son, Kwang Myong Lee, Parameters influencing water permeability coefficient of cracked concrete specimens, Constr. Build. Mater., 151.
[70] Jianwei Huang, Riyad Aboutaha, Environmental reduction factors for GFRP bars used as concrete reinforcement: new scientific approach, J. Compos. Constr. 14 (5) (2010).
[71] Tarek H. Almusallam, Yousef A. Al-Salloum, Saleh H. Alsayed, Sherif El-Gamal, Mohammed Aqel, Tensile properties degradation of glass fiber-reinforced polymer bars embedded in concrete under severe laboratory and field environmental conditions, J. Compos. Mater. 47 (4) (2012) 393–407.
[72] T.M. Chrisp, W.J. McCarter, G. Starrs, P.A.M. Basheer, J. Blewett, Depth-related variation in conductivity to study cover-zone concrete during wetting drying, Cem. Concr. Compos. 24 (2002) 415–426.
[73] M.A. Bérube, J.F. Doriona, J. Duchesnea, B. Fournier, D. Vézina, Laboratory and field investigations of the influence of sodium chloride on alkali–silica reactivity, Cem. Concr. Res. 33 (2003) 77–84.
[74] A. Lekatou, S.E. Faidi, D. Ghidaoui, S.B. Lyon, R.C. Newman, Effect of water and its activity on transport properties of glass/epoxy particulate composites, Compos. Part A 28 (3) (1997) 223–236.